ECN-RX--04-129

DYNAMIC INFLOW COMPENSATION FOR PITCH CONTROLLED WIND TURBINES

T.G. van Engelen

E.L. van der Hooft

This paper has been presented at the European Wind Energy Conference,

London, 22-25 November, 2004

NOVEMBER 2004

Dynamic Inflow Compensation for Pitch Controlled Wind Turbines

T.G. van Engelen, E.L. van der Hooft

Energy research Centre of the Netherlands (ECN), Wind Energy
P.O. Box 1, NL-1755 ZG Petten, The Netherlands
telephone: ++31 224 564141, telefax: ++31 224 568214
email: vanengelen@ecn.nl

ABSTRACT: An algorithm has been developed that provides filter parameters for pitch control loops in order to compensate for dynamic inflow effects. This improves the loop stability, especially near rated conditions. The filter behaviour reflects the 'inverse of the normalised' rotor-integral dynamic wake behaviour in accordance with the ECN differential equation wake model. Any (existing) pitch controller can be upgraded with such a filter. The algorithm has been implemented and incorporated in the ECN control design tool.

Keywords: Dynamic inflow, Pitch control, Improved stability.

1. INTRODUCTION

Research work on dynamic inflow pointed out that the measured short-term response of rotor loads on pitch variations may exceed the predicted loads from equilibrium wake aerodynamic analysis [1]. The effect appeared significant near rated conditions and was defined 'dynamic inflow'. In an earlier stage of pitch control development, the simulation of variable speed wind turbines with pitch-to-vane control in PHATAS [3] occasionally showed poor loop stability. Since this also occured near rated conditions it was assumed that this was caused by the (temporarily) higher 'process gain', that is to say the senstivity of the aerodynamic torque to pitch variation, as a result of dynamic inflow. This made us to look for a device that could compensate for the dynamic wake response on blade pitching in wind turbines. In addition, the parametrisation had to be convenient and the implementation as an 'add-on' to existing control algorithms was very desirable. Point of departure for the development of this 'compensation algorithm' was the dynamic inflow model of Snel and Schepers, called the 'ECN differential equation wake model' which had been derived from the 'ECN cylindrical wake model' [2].

2. APPROACH

The compensation method is based on a linearised treatment of the verified ECN differential equation wake model. More specifically, we derived filters for the pitch angle and the wind speed for use with $C_{\rm p}-$ and $C_{\rm t}$-data that cater for the transient effects in the rotor torque and thrust caused by the dynamic wake behaviour. In a working point, the transient dynamic behaviour of the rotor loads is modelled by a first order lead-lag filter $H_X^{\rm DI}$, with transfer function description:

$$H_X^{\rm DI}(s) = \frac{X^{\rm DI}(s)}{X^{\rm EquiWake}}(s) \quad = \quad \frac{(1+\tau_{\rm lead}^X(\mathrm{V_w},\Theta,\Omega))}{(1+\tau_{\rm lag}^X(\mathrm{V_w},\Theta,\Omega))} \tag{1}$$

Input to the filter is the aerodynamic torque $T_{\rm a}$ or thrust $F_{\rm a}$ that result from equilibrium wake aerodynamic conversion ($X^{\rm EquiWake}$). The filter output is the 'real' rotor load $X^{\rm DI}$ with the dynamic inflow effect included. The time constants $\tau_{\rm lead}^X$ and $\tau_{\rm lag}^X$ depend on the working point, defined by the wind speed $V_{\rm w}$, pitch angle Θ and rotor speed Ω. The larger the ratio between $\tau_{\rm lead}^X$ and $\tau_{\rm lag}^X$, the larger the ratio between the frozen wake (= 'short-term') and equilibrium wake response of the filter.

Figure 1 shows the dependency of the lead and lag time constants of the simplified dynamic wake model by Eq. (1) on the wind speed (the pitch angle and rotor speed vary in accordance with the 'working point trajectory' for rated power operation).

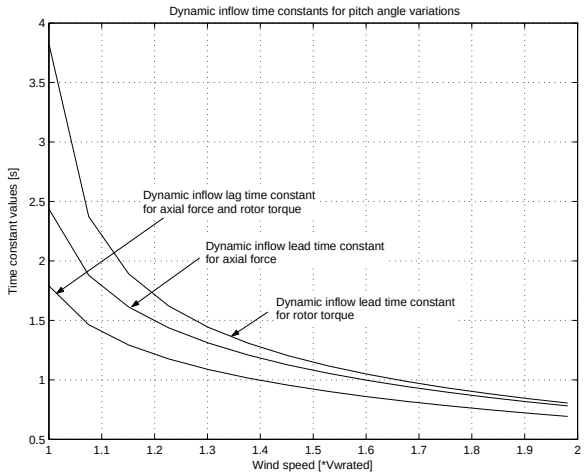

Figure 1: *Lead and lag time constants of Dynamic inflow modelling by Eq. (1)*

The dashed lines in the plots of figure 2 show the dynamic wake effects according to eq. 1 via the transient behaviour on a stepwise change in the pitch angle for two working points, viz. in rated wind speed and 20% above rated wind speed.

The compensation algorithm is ideally set up by the inverse of the dynamic wake modelling lead-lag filter (1). A convenient implementation is obtained by letting the compensation time constants only depend on the low pass filtered pitch angle $\overline{\Theta}$. The transfer function $H_{T_{\rm a}}^{\rm DIC}$ of the compensation filter for the aerodynamic torque is:

$$H_{T_{\rm a}}^{\rm DIC}(s) = \frac{T_{\rm a}^{\rm DI}(s)}{T_{\rm a}^{\rm EquiWake}(s)} \quad = \quad \frac{(1+\tau_{\rm lag}^{T_{\rm a}}(\overline{\Theta}))}{(1+\tau_{\rm lead}^{T_{\rm a}}(\overline{\Theta}))} \tag{2}$$

The solid lines in figure 2 show the compensation algorithm response according to eq. 2 on a stepwise change in the pitch

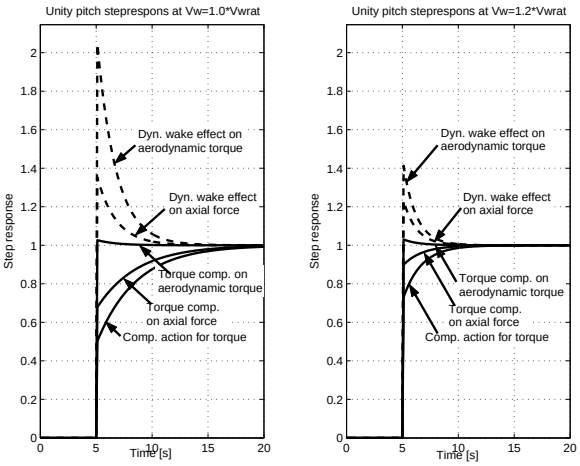

Figure 2: *Transient response of rotor loads via Eq. (1) and compensation algorithm output by Eq. (2)*

angle for the two working points. It can be observed that the product of the wake model and compensator responses equal 1.

3. DERIVATION OF FILTERS

The ECN differential wake model consists of annulus specific first order differential equations. In the linear area of the polars of the lift coefficients the induction behaviour in each annulus is governed by (U_i, R, c annulus axial induction speed, radius and chord, R_b blade radius):

$$2\pi R\Delta R\cdot\rho\cdot 2R_\mathrm{b}\cdot f_\mathrm{a}\cdot F_\mathrm{p}\cdot\tfrac{\mathrm{d}}{\mathrm{d}t}\big(U_\mathrm{i}\big)=B\cdot\tfrac{1}{2}\rho\cdot c\Delta R\cdot K\cdot (\arctan(\frac{V_\mathrm{w}-U_\mathrm{i}}{\Omega R})-\theta)\cdot\Omega R\cdot\sqrt{(\Omega R)^2+(V_\mathrm{w}-U_\mathrm{i})^2}- 2\pi R\Delta R\cdot\rho\cdot F_\mathrm{p}U_\mathrm{i}\cdot(V_\mathrm{w}-F_\mathrm{p}U_\mathrm{i}) \quad (3)$$

with Prandtl's tip correction factor F_p (as by [3]):

$$F_\mathrm{p} = \tfrac{4}{\pi^2}\cdot\arccos\big(\mathrm{e}^{-\frac{(R_\mathrm{b}-R)\pi}{d}}\big)\cdot\arccos\big(\mathrm{e}^{-\frac{(R-R_\mathrm{root})\pi}{d}}\big)$$

$$\text{with } d = \tfrac{2\pi R}{B}\cdot\frac{(V_\mathrm{w}-U_\mathrm{i})}{\sqrt{\big(\Omega\cdot R\big)^2+(V_\mathrm{w}-U_\mathrm{i})^2}}$$

The wake adaption factor f_a is proportioanl to reciprocal of speed of wake adaptation and decreases with increasing relative annulus radius R/R_b:

$$f_\mathrm{a}(R/R_\mathrm{b})=\frac{2\pi}{\displaystyle\int_0^{2\pi}\Big\{\frac{1-\big(\frac{R}{R_\mathrm{b}}\big)\cos\psi}{\big[1+\big(\frac{R}{R_\mathrm{b}}\big)^2-2\big(\frac{R}{R_\mathrm{b}}\big)\cos\psi\big]^{1.5}}\Big\}\,\mathrm{d}\psi}$$

(0.80, 0.59, 0.25 for $R/R_\mathrm{b}=0.5,\ 0.7,\ 0.9$)

The corresponding annulus specific expressions for the axial force and aerodynamic torque are ($K'=\frac{1}{2}\rho\cdot c\Delta R\cdot K$, $V_\mathrm{rel}=\sqrt{(\Omega R)^2+(V_\mathrm{w}-U_\mathrm{i})^2}$):

$$F_\mathrm{ax} = K'\cdot(\arctan(\frac{V_\mathrm{w}-U_\mathrm{i}}{\Omega R})-\theta)\cdot\Omega R\cdot V_\mathrm{rel} \quad (4)$$

$$T_\mathrm{w} = R\cdot K'\cdot(\arctan(\frac{V_\mathrm{w}-U_\mathrm{i}}{\Omega R})-\theta)\cdot(V_\mathrm{w}-U_\mathrm{i})\cdot V_\mathrm{rel}$$

Linearisation of the equations for the loads and the axial induction speed yields the following expressions:

$$\begin{aligned}\delta F_\mathrm{ax} &= K^\mathrm{fr}_{\mathrm{f}\theta}\cdot\delta\theta+K^\mathrm{fr}_\mathrm{fv}\cdot\delta V_\mathrm{w}+K_\mathrm{fu}\cdot\delta U_\mathrm{i}\\ \delta T_\mathrm{w} &= K^\mathrm{fr}_{\mathrm{t}\theta}\cdot\delta\theta+K^\mathrm{fr}_\mathrm{tv}\cdot\delta V_\mathrm{w}+K_\mathrm{tu}\cdot\delta U_\mathrm{i}\\ \tfrac{\mathrm{d}}{\mathrm{d}t}\big(U_\mathrm{i}\big) &= -A\cdot\delta U_\mathrm{i}+B_\theta\cdot\delta\theta+B_\mathrm{v}\cdot\delta V_\mathrm{w} \quad (5)\end{aligned}$$

Note that all coefficients depend on the annulus and the working point.

With the time-derivative operator notation ($\frac{\mathrm{d}}{\mathrm{d}t}$) for the variation in the axial induction speed,

$$\delta U_\mathrm{i}=\tfrac{B_\theta}{\frac{\mathrm{d}}{\mathrm{d}t}+A}\cdot\delta\theta+\tfrac{B_\mathrm{v}}{\frac{\mathrm{d}}{\mathrm{d}t}+A}\cdot\delta V_\mathrm{w}\ ,$$

the transfer function from the pitch angle variation to the thrust force variation is obtained by just replacing the operator $\frac{\mathrm{d}}{\mathrm{d}t}$ by the Laplace operator s from the expression below

$$\delta F_\mathrm{ax} = (K^\mathrm{fr}_{\mathrm{f}\theta}+K_\mathrm{fu}\cdot\frac{B_\theta}{A})\cdot\left(\frac{(\frac{1}{A+B_\theta\cdot K_\mathrm{fu}/K^\mathrm{fr}_{\mathrm{f}\theta}})\cdot\frac{\mathrm{d}}{\mathrm{d}t}+1}{\frac{1}{A}\cdot\frac{\mathrm{d}}{\mathrm{d}t}+1}\right)\cdot\delta\theta \quad (6)$$

Similar expressions hold for the aerodynamic torque as output and the wind speed as input. This yields four equilibrium-wake gains and unit-gain filters per annulus:

$$\begin{aligned}\delta F_\mathrm{ax} &= K^\mathrm{eq}_{\mathrm{f}\theta}\cdot\frac{\tau_{\mathrm{d}_{\mathrm{f}\theta}}\frac{\mathrm{d}}{\mathrm{d}t}+1}{\tau_\mathrm{i}\frac{\mathrm{d}}{\mathrm{d}t}+1}\cdot\delta\theta+K^\mathrm{eq}_\mathrm{fv}\cdot\frac{\tau_{\mathrm{d}_\mathrm{fv}}\frac{\mathrm{d}}{\mathrm{d}t}+1}{\tau_\mathrm{i}\frac{\mathrm{d}}{\mathrm{d}t}+1}\cdot\delta V_\mathrm{w}\\ \delta T_\mathrm{w} &= K^\mathrm{eq}_{\mathrm{t}\theta}\cdot\frac{\tau_{\mathrm{d}_{\mathrm{t}\theta}}\frac{\mathrm{d}}{\mathrm{d}t}+1}{\tau_\mathrm{i}\frac{\mathrm{d}}{\mathrm{d}t}+1}\cdot\delta\theta+K^\mathrm{eq}_\mathrm{tv}\cdot\frac{\tau_{\mathrm{d}_\mathrm{tv}}\frac{\mathrm{d}}{\mathrm{d}t}+1}{\tau_\mathrm{i}\frac{\mathrm{d}}{\mathrm{d}t}+1}\cdot\delta V_\mathrm{w}\end{aligned}$$

with (per annulus and working point)

$$\begin{aligned}K^\mathrm{eq}_{\mathrm{f}\theta} &= (K^\mathrm{fr}_{\mathrm{f}\theta}+K_\mathrm{fu}\cdot\tfrac{B_\theta}{A}) \text{ (etc.)}\\ \tau_{\mathrm{d}_{\mathrm{f}\theta}} &= \tfrac{1}{A+B_\theta\cdot K_\mathrm{fu}/K^\mathrm{fr}_{\mathrm{f}\theta}} \text{ (etc.)}\\ \tau_\mathrm{i} &= \tfrac{1}{A}\end{aligned}$$

Summation over the rotor annuli and the blades yeilds the rotor-integral impact of wake dynamics (N annuli):

$$\begin{aligned}\delta F_{\mathrm{ax}_\mathrm{rot}} &= B\sum_{n=1}^{N}\left\{K^\mathrm{eq}_{\mathrm{f}\theta}\frac{\tau_{\mathrm{d}_{\mathrm{f}\theta}}\frac{\mathrm{d}}{\mathrm{d}t}+1}{\tau_\mathrm{i}\frac{\mathrm{d}}{\mathrm{d}t}+1}\right\}_n\delta\theta+\left\{K^\mathrm{eq}_\mathrm{fv}\frac{\tau_{\mathrm{d}_\mathrm{fv}}\frac{\mathrm{d}}{\mathrm{d}t}+1}{\tau_\mathrm{i}\frac{\mathrm{d}}{\mathrm{d}t}+1}\right\}_n\delta V_\mathrm{w}\\ \delta T_{\mathrm{w}_\mathrm{rot}} &= B\sum_{n=1}^{N}\left\{K^\mathrm{eq}_{\mathrm{t}\theta}\frac{\tau_{\mathrm{d}_{\mathrm{t}\theta}}\frac{\mathrm{d}}{\mathrm{d}t}+1}{\tau_\mathrm{i}\frac{\mathrm{d}}{\mathrm{d}t}+1}\right\}_n\delta\theta+\left\{K^\mathrm{eq}_\mathrm{tv}\frac{\tau_{\mathrm{d}_\mathrm{tv}}\frac{\mathrm{d}}{\mathrm{d}t}+1}{\tau_\mathrm{i}\frac{\mathrm{d}}{\mathrm{d}t}+1}\right\}_n\delta V_\mathrm{w}\end{aligned}$$

Assumption on separation of gains and time constants ($\Sigma R=\sum_{m=1}^{N}R_m$):

$$\begin{aligned}\delta F_{\mathrm{ax}_\mathrm{rot}} &= B\sum_{n=1}^{N}\{K^\mathrm{eq}_{\mathrm{f}\theta}\}_n\frac{\frac{1}{\Sigma R}\cdot\sum_{n=1}^{N}\{R\cdot\tau_{\mathrm{d}_{\mathrm{f}\theta}}\}_n\frac{\mathrm{d}}{\mathrm{d}t}+1}{\frac{1}{\Sigma R}\cdot\sum_{n=1}^{N}\{R\cdot\tau_\mathrm{i}\}_n\frac{\mathrm{d}}{\mathrm{d}t}+1}\cdot\delta\theta+\ldots\\ &= K^\mathrm{eq}_{\mathrm{F}\theta}\cdot\frac{\tau_{\mathrm{d}_{\mathrm{F}\theta}}\frac{\mathrm{d}}{\mathrm{d}t}+1}{\tau_\mathrm{I}\frac{\mathrm{d}}{\mathrm{d}t}+1}\cdot\delta\theta+\ldots \quad (7)\end{aligned}$$

allows use of C_t-data with 2 unit-gain filters for $F_{\mathrm{ax}_\mathrm{rot}}$:

$$\begin{aligned}\theta_\mathrm{F} &= \frac{\tau_{\mathrm{d}_{\mathrm{F}\theta}}\frac{\mathrm{d}}{\mathrm{d}t}+1}{\tau_\mathrm{I}\frac{\mathrm{d}}{\mathrm{d}t}+1}\cdot\theta \text{ and } V_{\mathrm{w}_\mathrm{F}} = \frac{\tau_{\mathrm{d}_\mathrm{Fv}}\frac{\mathrm{d}}{\mathrm{d}t}+1}{\tau_\mathrm{I}\frac{\mathrm{d}}{\mathrm{d}t}+1}\cdot V_\mathrm{w}\\ F_{\mathrm{ax}_\mathrm{rot}} &= \tfrac{1}{2}\rho\pi R_b^2\cdot C_\mathrm{t}(\tfrac{\Omega R_\mathrm{b}}{V_{\mathrm{w}_\mathrm{F}}},\theta_\mathrm{F})\cdot V^2_{\mathrm{w}_\mathrm{F}} \quad (8)\end{aligned}$$

(similar for T_{wrot} with C_{p}-data)

The required parameters in each annulus are:

- frozen wake gains $K^{\mathrm{fr}}_{\mathrm{f}\theta}$, $K^{\mathrm{fr}}_{\mathrm{fv}}$, $K^{\mathrm{fr}}_{\mathrm{t}\theta}$, $K^{\mathrm{fr}}_{\mathrm{tv}}$
- force and torque sensitivities K_{fu}, K_{tu} to induction

  $\Rightarrow$ linearised load expressions from Eq. (4)
- induction-change transition parameter A
- induction-change input parameters B_θ, B_{v}

  $\Rightarrow$ linearised axial impulse equation from Eq. (3)

The linearised load expressions and impulse equation must be available for the working point values V_{w}, Ω, θ_{pt}, the working point & annulus specific values U_{i}, and the annulus specific data c, θ_{tw}, K, R, ΔR ($\theta = \theta_{\mathrm{pt}} + \theta_{\mathrm{tw}} \Leftrightarrow$ setting = pitch+twist), $K = \mathrm{d}C_\ell/\mathrm{d}\alpha$).

A generic procedure, which only requires the overall data P_{rat}, $V_{\mathrm{w_{rat}}}$, Ω, R_{b}, B, can be applied. Such a procedure

- assumes K (2π /rad) and relative spanwise C_{p}-distribution (e.g. equal power extraction efficiency);
- estimates chord/twist-data from rated conditions;
- calculates $\{\theta_{\mathrm{pt}}\}$ and $\{\{U_{\mathrm{i}}\}\}$ in V_{w}-range.

(working points only for α small ($\simeq$ 0.2 rad or less))

Of course, the application of a non-linear aerodynamic code will yield more accurate results for the required working point values of the axial induction speeds in the rotor annuli. However, the demanded accuracy on the time constants derived is not that high. An error of ca. 10% will not significantly affect the quality of the compensation algorithm, which is set-up from the 'inverse dynamic wake model equations' (see Eq. (1) and (2)).

4. RESULTS

Figure 3 shows a typical near-rated simulation for a multi-MW-size wind turbine. Though the results do not differ that much, it can be observed that the variations in the thrust force and aerodynamic torque are lower when the dynamic inflow compensation algorithm is added to the controller. In addition, the pitch actuation is significantly more smooth in case of compensation.

The impact of dynamic inflow compensation on the loop stability is much more significant. Figure 4 shows the so called 'open loop gain' of the pitch control loop for the rotor speed (Nyquist plots).

The distance from the O-mark on the x-axis to the intersection of the graphs with the x-axis is a measure for the robustness of the loop stability (gain margin). In general, a distance of 0.5 is considered sufficiently safe. That is to the say, the closed loop stability is still guaranteed when the effect of pitch variation on the rotor speed is twice as strong as expected during the design.

Another stability measure is the so-called phase margin. If the phase shift of the overall transfer from pitch variations

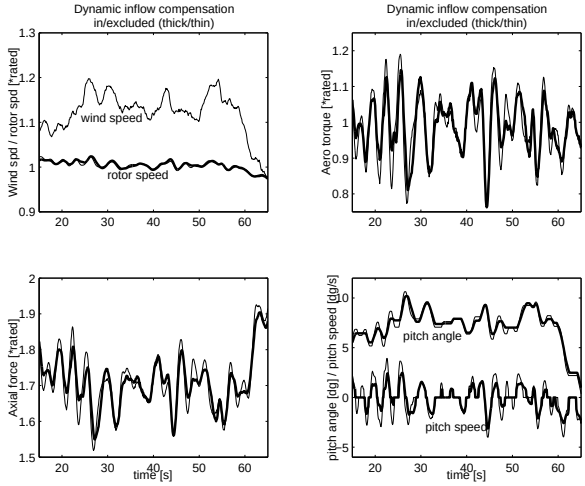

Figure 3: *Time domain simulation with and without dynamic inflow compensation*

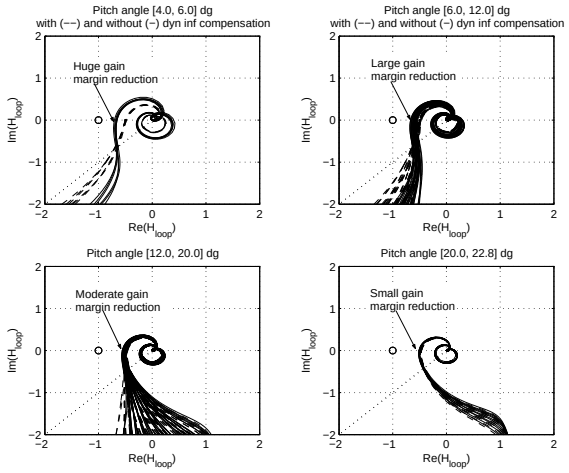

Figure 4: *Nyquist plots in four ranges of working points*

to the rotor speed variations is 45 degrees more in the upper bound of the controller bandwidth (e.g. 1.0 rad/s) than expected, stability is still guaranteed. Additional phase shift is caused by e.g. a slower responding pitch actuator than expected.

Especially near rated conditions (upper left plot), the stability margins are about half-size when dynamic inflow compensation is omitted. An implication of this is that an additional loop delay of ca. 0.2 s will yield instability while the allowed additional loop delay amounts to ca. 0.7 s when dynamic inflow compensation is included.

5. CONCLUSIONS

The developed compensation method for dynamic inflow reduces the complicated dynamics of the wake behaviour to a few simple differential equations. Incorporation in pitch control loops is straightforward and effective: a linear filter is added to a 'standard' pitch controller, designed on equilibrium wake aerodynamic data (like power and thrust coefficient data). It improves the loop stability around rated conditions without loss of control performance, slightly lowers the rotor

loads, and significantly lowers the pitch actuator load. The compensation algorithm can be elegantly parametrised with a stand-alone algorithm, which neither requires detailed turbine data nor simulations with an aerodynamic code. The filter is included in control algorithms [5] with satisfying results in simulations and in the field [4].

ACKNOWLEDGEMENT

The authors like to thank Koert Lindenburg for performing simulations with PHATAS focused on the dynamic inflow effect and the Netherlands Agency for Energy and the Environment NOVEM for funding of this resarch (contract 2020-12-10-003).

REFERENCES

[1] H. Snel, J.G. Schepers; *Joint Investigation of Dynamic Inflow Effects and Implementation of an Engineering Method*. Technical Report ECN-C-94-107, ECN Wind Energy, Petten, the Netherlands, April, 1995.

[2] H. Snel, J.G. Schepers; *Engineering Models for Dynamic Inflow Phenomena*, pg 267-281 in Journal of Wind Engineering and Industrial Aerodynamics, Elsevier Science Publ. Amsterdam, 1992.

[3] C. Lindenburg, J.T.G. Schepers, *PHATAS-IV Aeroelastic Modelling*, ECN-CX–00-027, ECN, the Netherlands.

[4] E.L. van der Hooft, P. Schaak, T.G. van Engelen, *Wind Turbine Control Algorithms: DOWEC-F1F1-EH-03-094/0*; ECN-C–03-111; ECN Windenrgie, Petten, December 2003.

[5] P. Schaak, T.G. van Engelen, E.L. van der Hooft, E.J. van Wiggelinkhuizen, *Development of a Wind Turbine Control Design Tool, Phase I (in Dutch)*; ECN-C–03-111; ECN Windenrgie, Petten, December 2003.